Model Investigations of Vanadium−Protein Interactions: Novel Vanadium(III) and Oxovanadium(IV) Compounds with the Diamidate Ligand 1,2-Bis(2-pyridinecarboxamide)benzene (H_2bpb)

Antonis T. Vlahos,[†] Evagelos I. Tolis,[†] Catherine P. Raptopoulou,[‡] Alexandros Tsohos,[‡] Michael P. Sigalas,*[,§] Aris Terzis,*[,‡] and Themistoklis A. Kabanos*[,†]

Department of Chemistry, Section of Inorganic and Analytical Chemistry, University of Ioannina, 451 10 Ioannina, Greece, NCSR "Demokritos", Institute of Materials Science, 15310 Aghia Paraskevi Attikis, Greece, and Laboratory of Applied Quantum Chemistry, Department of Chemistry, Aristotle University of Thessaloniki, 54006 Thessaloniki, Greece

Received July 14, 1999

Novel vanadium(III) and oxovanadium(IV) compounds with the diamidate ligand 1,2-bis(2-pyridinecarboxamide)-benzene (H_2bpb) were synthesized and structurally characterized. H_2bpb is capable of binding to vanadium in either its anionic (dianionic-monoanionic) or its neutral form, resulting in complexes of various geometries and stoichiometries. The dianionic form (bpb^{2-}), in $NHEt_3${*trans*-[VCl_2(bpb)]} (**1**) and [VO(bpb)(H_2O)]·0.5dmso·0.36CH_3-OH·0.13H_2O (**6**·0.5dmso·0.36CH_3OH·0.13H_2O), acts as a planar tetradentate bis[*N*-amidate-*N*-pyridine] equatorial ligand. The monoanionic form ($Hbpb^-$) behaves as an (N_{py},O_{am}) or (N_{py},N_{am}) chelator in [V($Hbpb)_3$]·2$CHCl_3$ (**2**·2$CHCl_3$) as well as a μ_2-bridging-η^4-(N_{py},O_{am}−N_{py},N_{am}) in [VOCl($Hbpb$)]$_2$·2CH_3NO_2 (**3**·2CH_3NO_2), while the neutral H_2bpb behaves as a μ^2-bridging-η^4-bis(N_{py},O_{am}) in [VOCl(H_2bpb)]$_2$·1.04CH_3OH·1.23thf·0.74H_2O (**4**·1.04CH_3OH·1.23thf·0.74H_2O). Compound **4**·1.04CH_3OH·1.23thf·0.74H_2O crystallizes in the triclinic system $P\bar{1}$, with (at 25 °C) a = 9.140(2) Å, b = 11.058(2) Å, c = 14.175(2) Å, α = 99.013(5)°, β = 104.728(7)°, γ = 102.992(7)°, V = 1314.9(4) Å^3, Z = 1, while compound **6**·0.5dmso·0.36CH_3OH·0.13H_2O crystallizes in the monoclinic space group $P2_1/n$ with (at 25 °C) a = 11.054(5) Å, b = 11.407(5) Å, c = 16.964(7) Å, β = 93.2(1)°, V = 2136(2) Å^3, Z = 4. Variable temperature magnetic susceptibility studies of the dimeric compounds **3**·2CH_3NO_2 and **4**·1.04CH_3OH show g values for the V(IV) centers that are slightly smaller than 2.0 (as expected for d^1 ions) and indicate small antiferromagnetic coupling between the two vanadium(IV) centers. Ab initio calculations were also carried out, providing results concerning the effect of the relative strength and the deformation energy involved in the η^2-(N_{py},N_{am}) and η^2-(N_{py},O_{am}) bonding modes in the ligation of $Hbpb^-$ to vanadium.

Introduction

Vanadium is a bioessential element that is found in remarkably high concentrations in marine ascidians,[1] in certain mushrooms,[2] and in polychaete worms,[3] but its role is still a mystery, although quite a few hypotheses have been presented. Moreover, the isolation and characterization of two families of vanadium-dependent enzymes, namely, of the nitrogenases[4] and the haloperoxidases,[5] as well as the ability of vanadium to produce significant physiological effects,[6] such as the increment in the cytosolic reduced glutathione[7] and glutathione S-transferase,[7] anticancer activity,[8] and in particular its insulin-like properties, etc.,[9] have stimulated further efforts in the development of the coordination chemistry and biochemistry of vanadium.[10] The synthesis as well as the structural and spectroscopic characterization of low molecular weight model complexes with the biologically important oxidation states (+II to +V) of vanadium will help in making further progress in the elucidation of biological role of vanadium.

Currently, we,[11] as well as others,[12] have been studying the interaction between vanadium and constituents of proteins,

[†] University of Ioannina.
[‡] Institute of Materials Science.
[§] Aristotle University of Thessaloniki.

(1) (a) Smith, M. J.; Kim, O.; Horenstein, B.; Nakanishi, K.; Kustin, K. *Acc. Chem. Res.* **1991**, *24*, 117. (b) Taylor, S. W.; Kammerer, B.; Bayer, E. *Chem. Rev.* **1997**, *97*, 333.
(2) (a) Koch, E.; Kneifel, H.; Bayer, E. *Z. Naturforsch., C* **1987**, *42*, 873. (b) Berry, R. E.; Armstrong, E. M.; Beddoes, R. L.; Collison, D.; Ertok, S. N.; Helliwell, M.; Garner, C. D. *Angew. Chem.* **1999**, *38*, 795.
(3) Ishii, T.; Nakai, I.; Numako, C.; Ohoshi, K.; Otake, K. *Naturwissenschaften* **1993**, *80*, 268.
(4) (a) Joerger, R. D.; Loveless, T. M.; Pau, R. N.; Mitchenal, L. A.; Simon, B. H.; Bishop, P. E. *J. Bacteriol.* **1990**, *172*, 3400. (b) Harvey, I.; Arber, J. M.; Eady, R. R.; Smith, B. E.; Garner, C. D.; Hasnain, S. S. *Biochem. J.* **1990**, *266*, 929. (c) Chen, J.; Christiansen, J.; Tittsworth, R. C.; Hales, B. J.; George, S. J.; Coucouvanis, D.; Cramer, S. P. *J. Am. Chem. Soc.* **1993**, *115*, 5509. (d) Vilter, H. In *Metal Ions in Biological Systems*; Sigel, H., A. Sigel, A.; Eds.; Marcel Decker: New York, 1995; Vol. 31, Chapter 10.
(5) (a) Schijndel, V.; Barnett, J. W. P. M. P.; Roelse, J.; Vollenbroek, E. G. M.; Wever. R. *Eur. J. Biochem.* **1994**, *225*, 151. (b) Messerschmidt, A.; Wever, R. *Proc. Natl. Acad. Sci. U.S.A.* **1996**, *93*, 392. (c) Macedo-Ribeiro, S.; Hemrika, W.; Revirie, R.; Wever, R.; Messerschmidt, A. *J. Biol. Inorg. Chem.* **1999**, *4*, 209. (d) Eedy, R. R.; Leigh, G. J. *J. Chem. Soc., Dalton Trans.* **1994**, 2739. (e) Eedy, R. R. In *Metal Ions in Biological Systems*; Sigel, H., Sigel, A., Eds.; Marcel Decker: New York, 1995; Vol. 31, Chapter 11.
(6) (a) Stankiewicz, P. J.; Tracey, A. S.; Crans, D. C. In *Metal Ions in Biological Systems*; Sigel, H., Sigel, A., Eds.; Marcel Decker: New York, 1995; Vol. 31, Chapters 8 and 9. (b) Etcheverry, S. B.; Cortizo, A. M. In *Vanadium in the Environment*; Nriagu, J. O., Ed.; John Wiley and Sons: New York, 1998; Vol. 30, Chapter 15.
(7) Bishayee, A.; Chatterjee, M. *Biol. Trace Elem. Res.* **1995**, *48*, 275.
(8) (a) Nagar, M. M.; Wassef, A. M.; Halafawy, K. M.; Sayed, I. H. *Cancer Lett.* **1998**, *133*, 71. (b) Liasko, R.; Kabanos, T. A.; Karkabounas, S.; Malamas, M.; Tasiopoulos, A. J.; Stefanou, D.; Collery, P.; Evangelou, A. *Anticancer Res.* **1998**, *18*, 3609.

10.1021/ic990837z CCC: $19.00
Published on Web 06/17/2000

namely, amides, amino acid amides, and peptides. These systems serve as models of the interaction between metal centers of metalloenzymes and the amide group of their peptide substrates. Our studies are undertaken in the hope that a better understanding of the interaction between vanadium species, and more generally transition metal ions, and proteins will be achieved.

A literature survey, for the diamidate ligand H_2bpb, revealed that in almost all the crystallographically characterized H_2bpb−metal compounds, the ligand acts as a dianionic planar bis[*N*-amidate-*N*-pyridine] chelator.[13] To this trend, there are only two exceptions.[14] Metal−bpb^{2-} compounds have been used as epoxidation[13d,15] or hydroxylation[16] catalysts. Herein, we wish to report the synthesis and structural characterization of novel vanadium(III) and oxovanadium(IV) compounds with H_2bpb, Hbpb$^-$, and bpb^{2-}. In addition, infrared and variable temperature magnetic susceptibility properties of the complexes are reported. Furthermore, an ab initio study of the Hbpb$^-$ ligand and of the two model complexes of the general formula $[VCl_2(NH_3)_2$(Hbpb)] is reported. A special emphasis is placed on understanding the energetics of the ligation of Hbpb$^-$ in its η^2-(N_{py},O_{am}) or η^2-(N_{py},N_{am}) coordination modes. The structures of **1**, **2**·2$CHCl_3$, and **3**·2CH_3NO_2 (vide infra) have previously been communicated.[17]

Experimental Section

Materials. Reagent grade chemicals were obtained from Aldrich and used without further purification. Dichlorobis(tetrahydrofuran)-oxovanadium(IV), $[VOCl_2(thf)_2]$,[18] tris(acetonitrile) trichlorovanadium-(III), $[VCl_3(CH_3CN)_3]$,[19] bis(acetato)oxovandium(IV), $[VO(CH_3COO)_2]_x$,[20] and 1,2-bis(2-pyridinecarboxamide)benzene, H_2bpb,[21] were prepared according to literature procedures. The purity of the above molecules was confirmed by elemental analyses (C, H, N, and V for vanadium compounds) and infrared spectroscopy. Reagent grade dichloromethane, chloroform, acetonitrile, nitromethane, thiethylamine, isopropyl alcohol, and dimethylformamide were dried and distilled (dimethylformamide was distilled under reduced pressure) over calcium hydride, while toluene, diethyl ether, and tetrahydrofuran were dried and distilled over sodium wire. Methyl alcohol was dried by refluxing over magnesium methoxide. Syntheses, distillations, crystallization of the complexes, and spectroscopic characterization were performed under high-purity argon using standard Schlenk techniques.

C, H, and N analyses were conducted by the University of Ioannina's microanalytical service. Vanadium was determined gravimetrically as vanadium pentoxide or by atomic absorption, and chloride analyses were carried out by potentiometric titration.

Triethylammonium *trans*-Dichloro{1,2-bis(2-pyridinecarboxamide)benzenato(−2)-η^4-N_{py},N_{am},N_{am},N_{py}}vanadate(III), $NHEt_3$-{*trans*-$[VCl_2(bpb)]$} (1). Method A. A stirred mixture of vanadium-(III) chloride (0.428 g, 2.73 mmol), H_2bpb (0.868 g, 2.73 mmol), and triethylamine (1.38 g, 13.6 mmol) in toluene (50 mL) was refluxed overnight. The resulting brick-red precipitate, which is a mixture of **1**, $[VO(bpb)]_x$, and $NHEt_3Cl$, was filtered off and washed with diethyl ether (3 × 10 mL) and dried in vacuo. The solid was extracted with dichloromethane (∼50 mL) and then the solvent removed to give a red solid. The residual solid was redissolved in chloroform (∼40 mL) and filtered, and 40 mL of diethyl ether was very carefully layered on top of the filtrate and cooled to −20 °C for 3 days to give dark-red and white crystals that were filtered off and dried in vacuo. The dark-red crystals were manually separated readily under a microscope. Yield: 0.148 g (10%). Anal. Calcd for $C_{24}H_{28}Cl_2N_5O_2V$: C, 53.35; H, 5.22; Cl, 13.12; N, 12.96; V, 9.43. Found: C, 53.30; H, 5.19; Cl, 13.00; N, 13.02; V, 9.40. μ_{eff} = 2.75 μ_B at 298 K. Electronic spectrum in CH_2Cl_2, λ_{max}, nm (ϵ_M, L mol^{-1} cm^{-1}): 220 (22 900), 261 (17 700), 290(sh) (9200), 349 (7700); in CH_3CN, 197 (39 000), 204(sh) (36 000), 259 (20 400), 284(sh) (9000), 350 (9300).

Method B. To a stirred solution of $[VCl_3(CH_3CN)_3]$ (1.340 g, 8.540 mmol) in acetonitrile (60 mL) was added in one portion solid H_2bpb (2.730 g, 8.540 mmol). The color immediately changed from dark-green to very light-green, and a light-green solid precipitated. The mixture was stirred for ∼5 min before thiethylamine (1.980 g, 19.60 mmol) was added to it. The color of the solution immediately changed to dark-brown. After about 2 h of stirring at ambient termperature, the solution was filtered off. The residue was extracted with CH_3CN (∼30 mL). The extract was combined with the filtrate and was evaporated in vacuo to dryness. The residual solid was redissolved in dichloromethane (∼45 mL), the solution filtered and concentrated (∼15 mL), diethyl ether (∼45 mL) was added dropwise to the stirred filtrate, and the resulting precipitate was filtered off, washed with diethyl ether (2 × 10 mL), and dried in vacuo. The precipitate was triturated with cold isopropyl alcohol (2 × 30 mL) at ambient temperature, filtered off, washed with diethyl ether (2 × 10 mL), and dried in vacuo. Yield: 2.77 g (60%).

(9) (a)Shaver, A.; Ng, J. B.; Hall, O. A.; Lum, B. S.; Posner, B. I. *Inorg. Chem.* **1993**, *32*, 3109. (b) Watanabe, H.; Nakai, M.; Komazawa, K.; Sakurai, H. *J. Med. Chem.* **1994**, *37*, 876. (c) Caravan, P.; Gelmini, L.; Glover, N.; Herring, F. G.; Li, H.; McNeil, J. H.; Retting, S. J.; Setyawati, I. A.; Shuter, E.; Sun, Y.; Tracey, A. S.; Yuen, V. G.; Orvig, C. *J. Am. Chem. Soc.* **1995**, *117*, 12759. (d) Crans, D. C.; Keramidas, A. D.; Hoover-Litty, H.; Anderson, O. P.; Miller, M. M.; Lemoine, L. M.; Pleasu-Williams, S.; Vandenberg, M.; Rossomando, A. J.; Sweet, L. J. *J. Am. Chem. Soc* **1997**, *199*, 55447. (e) Sakurai, H.; Watanabe, H.; Tamura, H.; Yasui, H.; Matsushita, R.; Takada, J. *Inorg. Chim. Acta* **1998**, *283*, 175.

(10) (a) Rehder, D. In *Metal Ions in Biological Systems*; Sigel, H., Sigel, A., Eds.; Marcel Decker: New York, 1995; Vol. 31, Chapter 1. (b) Rehder, D.; Jantzen, S. In *Vanadium in the Environment*; Nriagu, J. O., Ed.; John Wiley and Sons: New York, 1998; Vol. 30, Chapter 11. (c) Rehder, D. *Coord. Chem. Rev.* **1999**, *182*, 297.

(11) (a) Keramidas, A. D.; Papaioannou, A. B.; Vlahos, A.; Kabanos, T. A.; Bonas, G.; Makriyannis, A.; Raptopoulou, C. P.; Terzis, A. *Inorg. Chem.* **1996**, *35*, 357. (b) Tasiopoulos, A. J.; Vlahos, A. T.; Keramidas, A. D.; Kabanos, T. A.; Deligiannakis, Y. G.; Raptopoulou, C. P.; Terzis, A. *Angew. Chem., Int. Ed. Engl.* **1996**, *35*, 253. (c) Tasiopoulos, A. J.; Deligiannakis, Y. G.; Woollins, J. D.; Slawin, A. M.; Kabanos, T. A. *Chem. Commun.* **1998**, 569. (d) Soulti, K. D.; Troganis, A.; Papaioannou, A.; Kabanos, T. A.; Keramidas, A. D.; Deligiannakis, Y. G.; Raptopoulou, C. P.; Terzis, A. *Inorg. Chem.* **1998**, *37*, 6785. (e) Tasiopoulos, A. J.; Troganis, A. N.; Evangelou, A.; Raptopoulou, C. R.; Terzis, A.; Deligiannakis, Y.; Kabanos, T. A. *Chem.—Eur. J.* **1999**, *5*, 910.

(12) (a) Borovic, A. S.; Dewey, T. M.; Raymond, K. N. *Inorg. Chem.* **1993**, *32*, 413. (b) Cornman, C. R.; Zovinka, E. P.; Boyajian, Y. D.; Geiser-Bush, K. M.; Boyle, P. D.; Singh, P. *Inorg. Chem.* **1995**, *34*, 4213. (c) Einstein, F. W. B.; Batchelor, R. J.; Angus-Dunne, S. J.; Tracey, A. S. *Inorg. Chem.* **1996**, *35*, 1680. (d) Keramidas, A. D.; Miller, S. M.; Anderson, O. P.; Crans, D. C. *J. Am. Chem. Soc.* **1997**, *119*, 8901. (e) Hamstra, B. J.; Houseman, L. P.; Colpas, G. J.; Kampf, J. W.; LoBrutto, R.; Frasch, W. D.; Pecoraro, V. L. *Inorg. Chem.* **1997**, *36*, 4866. (f) Colpas, G. J.; Hamstra, B. J.; Kampf, J. W.; Pecoraro, V. L. *J. Am. Chem. Soc.* **1996**, *118*, 3469. (g) Kiss, T.; Petrohan, K.; Buglyo, P.; Sanna, D.; Micera, G.; Pessoa, J. C.; Madeira, C. *Inorg. Chem.* **1998**, *37*, 7, 6389.

(13) (a) Yang, Y.; Diederich, F.; Valentine, J. S. *J. Am. Chem. Soc.* **1991**, *113*, 7195. (b) Mak, S.; Wong, W.; Yam, V. W.; Lai, T.; Che, C. *J. Chem. Soc., Dalton Trans.* **1991**, 1915. (c) Mak, S.; Yam, V. M.; Che, C. *J. Chem. Soc., Dalton Trans.* **1990**, 2555. (d) Stephens, F. S.; Vagg, R. S. *Inorg. Chim. Acta* **1986**, *120*, 165. (e) Che, C.; Cheng, W.; Mak, T. C. W. *J. Chem. Soc., Chem. Commun.* **1986**, 200. (f) Chapman, R. L.; Stephens, F. S.; Vagg, R. S. *Inorg. Chim. Acta* **1980**, *43*, 29.

(14) (a) Cornman, C. R.; Zovinka, E. P.; Boyajian, Y. D.; Olmstead, M. M.; Noll, B. C. *Inorg. Chim. Acta* **1999**, *285*, 134. (b) Leung, W.; Hun, T. S. M.; Hui, K.; Williams, I. D.; Vanderveer, D. *Polyhedron* **1996**, *15*, 421.

(15) Ray, M.; Mukherjee, R.; Richardson, J. F.; Buchanan, R. M. *J. Chem. Soc., Dalton Trans.* **1993**, 2451.

(16) Saussine, L.; Brazi, E.; Robine, A.; Mimann, H.; Fisher, J.; Weiss, R. *J. Am. Chem. Soc.* **1985**, *107*, 4.

(17) Vlahos, A. T.; Kabanos, T. A.; Raptopoulou, C. P.; Terzis, A. *Chem. Commun.* **1997**, 269.

(18) Kern, R. *J. Inorg. Nucl. Chem.* **1962**, *24*, 1105.

(19) Casey, A. T.; Clark, R. J.; Nyholm, R. S.; Scaife, D. E. *Inorg. Synth.* **1972**, *13*, 165.

(20) Chand-Paul, R.; Bathia, S.; Kumar, A. *Inorg. Synth.* **1982**, *13*, 181.

(21) Barnes, D. J.; Chapman, R. L.; Vagg, R. S.; Watton, E. C. *J. Chem. Eng. Data* **1978**, *23*, 349.

Table 1. Summary of Crystal and Refinement Data for Complexes **4**·1.04CH_3OH·1.23thf·0.74H_2O and **6**·0.5dmso·0.36CH_3OH·0.13H_2O

	4·1.04CH_3OH·1.23thf·0.74H_2O	**6**·0.5dmso·0.36CH_3OH·0.13H_2O
empirical formula	$C_{41.96}H_{43.48}N_8O_{9.01}Cl_4V_2$	$C_{19.36}H_{18.7}N_4O_{4.99}S_{0.5}V$
fw	1047.71	454.22
temp,K	298	298
wavelength, Å, source	1.5418, Cu Kα	0.71073, Mo Kα
cryst symmetry	triclinic	monoclinic
space group	$P\bar{1}$	$P2_1/n$
a, Å	9.140(2)	11.054(5)
b, Å	11.058(2)	11.407(5)
c, Å	14.175(2)	16.964(7)
α, deg	99.013(5)	
β, deg	104.728(7)	93.21(1)
γ, deg	102.992(7)	
V, Å^3	1314.9(4)	2136(2)
Z	1	4
d_{calcd}/d_{measd}, g cm^{-3}	1.416/1.40	1.438/1.42
μ, mm^{-1}	5.16	0.562
F(000)	537	935
goodness of fit	1.066	1.050
R1	0.0638[a]	0.0485[b]
wR2	0.1627[a]	0.1398[b]

[a] For 2491 refs $I > 2\sigma(I)$. [b] For 3500 refs $I > 2\sigma(I)$.

Bis[1,2-bis(2-pyridinecarboxamide)benzenato(−1)-η^2-N_{py},O_{am}]-[1,2-bis(2-pyridine-carboxamide)benzenato(−1)-η^2-N_{py},N_{am}]vanadium-(III), [V(Hbpb)$_3$]·2$CHCl_3$ (2·2$CHCl_3$). Gaseous ammonia was bubbled in a stirred solution of toluene (∼60 mL) containing vanadium(III) chloride (0.980 g, 6.28 mmol) and H_2bpb (2.000 g, 6.28 mmol). The solution was refluxed for 10 h, after which a brick-red precipitate was formed. The precipitate was filtered off, washed with hot toluene (3 × 10 mL) and diethyl ether (2 × 10 mL), and dried in vacuo. The solid was extracted with dichloromethane (∼15 mL), filtered, and evaporated to dryness under reduced pressure, resulting in 0.20 g of solid. When diethyl ether was layered into a concentrated chloroform solution of the solid, brick-red crystals were isolated. One of these crystals proved to be **2**·2$CHCl_3$. A high-yield synthesis of this material has not been determined to date.

Bis{[1,2-bis(2-pyridinecarboxamide)benzenato(−1)-μ_2-η^4-N_{py},O_{am}-N_{py},N_{am}]-*cis*-chlorooxovanadium(IV)}, [VOCl(Hbpb)]$_2$·2CH_3NO_2 (3·2CH_3NO_2). Complex **1** (0.545 g, 1.00 mmol) was dissolved in nitromethane (10 mL). The resulting red solution was filtered off and the filtrate left in the atmosphere under magnetic stirring for 3 days after which the color of the solution changed to light-green and a green precipitate was formed. The green solid was filtered off, washed with nitromethane (2 × 10 mL) and diethyl ether (2 × 15 mL), and dried in vacuo to yield 0.42 g (87%) of product. Anal. Calcd for $C_{36}H_{26}Cl_2N_4O_6V_2$·2$CH_3NO_2$: C, 47.46; H, 3.35; Cl, 7.37; N, 14.57; V, 10.59. Found: C, 47.43; H, 3.38; Cl, 7.30; N, 14.60; V, 10.63. Green crystals of **3** were obtained by dissolving 0.10 g of the complex in ∼10 mL of nitromethane and exposing the solution to the atmosphere.

Bis{[1,2-bis(2-pyridinecarboxamide)benzene-μ_2-η^4-(N_{py},O_{am})$_2$]-*cis*-chlorooxovanadium(IV)} Chloride, [VOCl(H$_2$bpb)]$_2$Cl$_2$·2thf (4·2thf). To a stirred solution of [$VOCl_2$(thf)$_2$] (1.330 g, 4.71 mmol) in tetrahydrofuran (40 mL) was added in one portion solid H_2bpb (1.500 g, 4.71 mmol). Upon addition of the ligand the blue solution turned to almost colorless and a light-green precipitate was formed. The stirring was continued for ∼1 h. The solid was filtered off, washed with tetrahydrofuran (2 × 10 mL) and diethyl ether (2 × 10 mL), and dried in vacuo to yield 2.06 g (96%) of product. Anal. Calcd for $C_{36}H_{28}Cl_4N_8O_6V_2$·2thf: C, 50.02; H, 4.20; Cl, 13.40; N, 10.60; V, 9.64. Found: C, 49.80; H, 4.30; Cl, 13.40; N, 10.54; V, 9.65. Crystals of **4**·1.04CH_3OH·1.23thf·0.74H_2O suitable for X-ray structure analysis were obtained by very slow diffusion of [$VOCl_2$(thf)$_2$] in methyl alcohol into a solution of H_2bpb in tetrahydrofuran. The elemental analysis of the crystals was not possible because of the solvent loss.

[1,2-Bis(2-pyridinecarboxamide)benzenato-η^4-N_{py},N_{am},N_{am},N_{py})]-oxovanadium(IV), [VO(bpb)]·CH_3OH (5·CH_3OH). Method A. To a stirred solution of [$VOCl_2$(thf)$_2$] (0.261 g, 0.92 mmol) in methyl alcohol (∼10 mL) was added in one portion solid H_2bpb (0.294 g, 0.92 mmol). Upon addition of the ligand the blue-green color of the solution changed to bright-green. Then triethylamine (0.95 g, 9.2 mmol) was added to it. An immediate color change to pale-yellow concurrent with the precipitation of an orange-brown solid was observed. The mixture was refluxed for 5 h. Then the solid was filtered off, washed with methyl alcohol (2 × 10 mL) and diethyl ether (2 × 15 mL), and dried in vacuo to yield 0.28 g of an orange product. Yield, 80%. Anal. Calcd for $C_{18}H_{12}N_4O_3V$·CH_3OH: C, 54.95; H, 3.88; N, 13.49; V, 12.27. Found: C, 54.75; H, 3.65; N, 13.52; V, 12.24. $\mu_{eff} = 1.95\ \mu_B$ at 298 K.

Method B. [$VO(CH_3COO)_2$] (0.692 g, 3.74 mmol) was partially dissolved in hot dimethylformamide (∼5 mL). Then the solution was cooled to room temperature and solid H_2bpb (1.192 g, 3.74 mmol) was added to it under magnetic stirring. The dark blue-green color of the solution changed to light-green. The mixture was refluxed for 2 h and the resulting orange-brown solid was filtered off, washed with methyl alcohol (2 × 10 mL) and diethyl ether (2 × 15 mL), and dried in vacuo. Yield, 1.08 g (75%). Anal. Calcd for $C_{18}H_{12}N_4O_3V$: C, 56.41; H, 3.16; N, 14.62; V, 13.29. Found: C, 56.42; H, 3.23; N, 14.50; V, 13.26.

[1,2-Bis(2-pyridinecarboxamide)benzenato(−2)-$\eta^4$$N_{py}$,$N_{am}$,$N_{am}$,$N_{py}$)]-*trans*-(aquo)oxovanadium(IV), [VO(bpb)(H$_2$O)]·0.5dmso·0.36CH_3OH·0.13H_2O (6·0.5dmso·0.36CH_3OH·0.13H_2O). Complex **5**·CH_3OH was dissolved in dimethyl sulfoxide and left in the air. After about a month green crystals of **6**·0.5dmso·0.36CH_3OH·0.13H_2O suitable for X-ray structure analysis were formed. Anal. Calcd for $C_{18}H_{14}N_4O_4V$·0.5dmso·0.36CH_3OH·0.13H_2O: C, 51.20; H, 4.15; N, 12.33; S, 3.53; V, 11.22. Found: C, 51.01; H, 4.20; N, 12.55; S, 3.60; V, 11.20.

Structure Determination for Compounds 4·1.04CH_3OH·1.23thf·0.74H_2O and 6·0.5dmso·0.36CH_3OH·0.13H_2O. A green prismatic crystal of **4**·1.04CH_3OH·1.23thf·0.74H_2O with dimensions 0.10 mm × 0.20 mm × 0.50 mm was mounted in a capillary with drops of the mother liquor because the crystals were very sensitive to air exposure. The crystal was not of the best quality, having large ω half-widths as well as asymmetric peaks with small shoulders on either side. Repeated efforts to improve the quality of the crystals did not prove to be successful. A green prismatic crystal of **6**·0.5dmso·0.36CH_3OH·0.13H_2O with dimensions 0.10 mm × 0.20 mm × 0.35 mm was mounted in air. Diffraction measurements for **4** and **6** were made on a $P2_1$ Nicolet diffractometer using Ni-filtered Cu Kα radiation and on a Crystal Logic Dual goniometer diffractometer using graphite monochromated Mo Kα radiation, respectively. Unit cell dimensions were determined and refined by using the angular settings of 25 automatically centered reflections in the range $24° < 2\theta < 54°$ (for **4**) and $11° < 2\theta < 23°$ (for **6**), and they appear in Table 1 along with other crystallographic data. Lorentz polarization and ψ-scan absorption corrections were applied using Crystal Logic software. Intensity data were recorded using a $\theta-2\theta$ scan. Details of data collection for **4**: scan speed 1.5°/

min; scan range 2.5 + $\alpha_1\alpha_2$ separation; $2\theta_{max} = 118°$; reflections collected/unique/used, 4063/3780 ($R_{int} = 0.0306$)/3766; 465 parameters refined; $[\Delta\rho]_{max}/[\Delta\rho]_{min} = 0.517/-0.466$ e/Å^3; $[\Delta/\sigma]_{max} = 0.189$; R1/wR2 (for all data) = 0.1068/0.1976. Details of data collection for **6**: scan speed 3.0°/min; scan range 2.5 + $\alpha_1\alpha_2$ separation; $2\theta_{max} = 52°$; reflections collected/unique/used, 4331/4189 ($R_{int} = 0.0096$)/4189; 351 parameters refined; $[\Delta\rho]_{max}/[\Delta\rho]_{min} = 0.690/-0.370$ e/Å^3; $[\Delta/\sigma]_{max} = 0.046$; R1/wR2 (for all data) = 0.0585/0.1512. The structures were solved by direct methods using SHELXS-86[22a] and refined by full-matrix least-squares techniques on F^2 with SHELXL-93.[22b] All hydrogen atoms in both **4** and **6** were located by difference Fourier maps and refined isotropically, while all non-hydrogen atoms were refined anisotropically. The oxo and chloro ligands in **4** were disordered over two positions with occupation factors 0.81 and 0.19, respectively. During the discussion we will be referring to the position with the high occupancy. During the refinement of **4**, problems with the crystallization solvents appeared, which were handled as follows. The methyl alcohol was disordered over three positions around the center of symmetry with the sum of their occupation factors being ~0.52. The disordered thf molecule was refined in two positions with the sum of the two occupation factors refining to ~0.6 (all atoms were refined anisotropically and hydrogen atoms included at calculated positions as riding on carbon atoms), and the water molecule was refined anisotropically with the occupation factor refining to a value of ~0.37. Compound **6** crystallizes from a mixture of solvents, in particular dimethyl sulfoxide, methyl alcohol, and water. Unfortunately, all these molecules appear in a disordered fashion in the asymmetric unit. We succeeded in assigning these peaks in the difference Fourier map and determining the presence of dmso, CH_3OH, and H_2O with occupation factors refined to 0.50, 0.36, and 0.13, respectively, per asymmetric unit. Solvent atoms (except for the methyl groups of dmso and the water molecule) were refined anisotropically. Hydrogen atoms of the solvents were not included in the refinement.

Physical Measurements. IR spectra were recorded on a Perkin-Elmer Spectrum G-X FT-IR system in KBr pellets or Nujol. Electronic absorption spectra were measured as solutions in septum-sealed quartz cuvettes on a Jasco V570 UV/vis/NIR spectrophotometer. Solution conductivity data were collected in dichromethane and acetonitrile using a Tacussel electronique CD 6NG conductivity bridge. A temperature of 25 °C was maintained by a constant-temperature bath. The cell constant was determined to be $\kappa = 1.1025$ cm^{-1} by using a 0.1 M aqueous solution of potassium chloride to calibrate the conductivity cell. Magnetic moments were measured at room temperature by the Faraday method, with mercuric tetrathiocyanatocobaltate(II) as the susceptibility standard on a Cahn-Vetron RM-2 balance. Variable-temperature magnetic susceptibility measurements were carried out on powdered samples of **3**·2CH_3NO_2 and **4**·2thf in the 3−300 K and 5−300 K temperature range, respectively, using a Quantum Design superconducting quantum interference device (SQUID) susceptometer in a 6.0 kG applied magnetic field. Electron paramagnetic resonance (EPR) spectra were recorded on a Bruker ER 2000D-SRC X-band spectrometer with an Oxford ESR 9 cryostat.

Computational Details. All calculations were carried out using an ab initio method at the Hartree−Fock (HF) SCF level. For the vanadium atom the effective core potential of Hay and Wadt,[23] which includes the 3s and 3p electrons in the valence shell, was chosen, while for H, K C, N, O, and Cl atoms the STO-3G basis set[24,25] was used. Molecular geometries of the ligands and of the model complexes were fully optimized at the HF level, using an analytical gradient technique with residual forces less than 5×10^{-4} hartree/bohr. All calculations were performed with the Gaussian 94 package[26] on an HP9000/J210 workstation.

Scheme 1. Synthesis of the Vanadium(III) and Oxovanadium(IV) Compounds with H_2bpb[a]

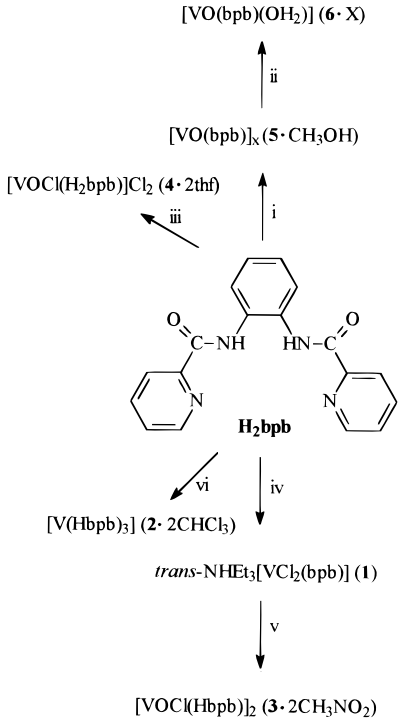

[a] Conditions: i, $[VOCl_2(thf)_2]$, Et_3N, CH_3OH, argon, reflux; ii, dmso, air, where X = 0.5dmso·0.3CH_3OH·0.13H_2O; iii, $[VOCl_2(thf)_2]$, thf, argon; iv, $[VCl_3[CH_3CN)_3]$, Et_3N, CH_3CN, argon; v, CH_3NO_2, air; vi, VCl_3, NH_3, toluene, reflux.

Results and Discussion

Synthesis of the Compounds. The synthesis of the vanadium(III) and oxovanadium(IV) compounds with the ligand H_2bpb is summarized in Scheme 1. Reaction of an equivalent of H_2bpb with an equivalent of VCl_3 and 5 equiv of triethylamine in toluene (reflux) for 14 h yielded a brick-red precipitate. The brick-red solid was a mixture of **1**, $[VO(bpb)]_x$,[27] and $NHEt_3$-Cl. Extraction of the solid with chloroform and layering diethyl ether on the top of it at −20 °C gave a mixture of dark-red crystals of **1** (which were manually separated) as well as white crystals of $NHEt_3Cl$. The yield was very low, ~10% (method A). In an effort to increase the yield of **1**, the same reaction was repeated in acetonitrile, where the reaction time was ~2 h at room temperature. Under these mild conditions, there was no oxidation of **1** to $[VO(bpb)]_x$ from atmospheric oxygen, thus resulting in a substantial increase of the yield (60%) of **1**. Substitution of gaseous ammonia (bubbling) for triethylamine in method A resulted in the formation of a very small quantity of brick-red crystals. One of the brick-red crystals formed proved to be, by X-ray structure analysis, **2**·2$CHCl_3$. A high-yield

(22) (a) Sceldrick, G. M. *SHELXS-86: Structure Solving Program*; University of Gottingen: Gottingen, Germany, 1986. (b) Sceldrick, G. M. *SHELXS-93: Crystal Structure Refinement*; University of Gottingen: Gottingen, Germany, 1993.
(23) Hay, P. J.; Wadt, W. R. *J. Chem. Phys.* **1985**, *82*, 299.
(24) Hehre, W. J.; Stewart, R. F.; Pople, J. A. *J. Chem. Phys.* **1969**, *51*, 2657.
(25) Collins, J. B.; Schleyer, P. v. R.; Binkley, J. S.; Pople, J. A. *J. Chem. Phys.* **1976**, *64*, 5142.
(26) Frisch, M. J.; Trucks, G. W.; Schlegel, H. B.; Gill, P. M. W.; Johnson, B. G.; Robb, M. A.; Cheeseman, J. R.; Keith, T.; Petersson, G. A.; Montgomery, J. A.; Raghavachari, K.; Al-Laham, M. A.; Zakrzewski, V. G.; Ortiz, J. V.; Foresman, J. B.; Cioslowski, J.; Stefanov, B. B.; Nanayakkara, A.; Challacombe, M.; Peng, C. Y.; Ayala, P. Y.; Chen, W.; Wong, M. W.; Andres, J. L.; Replogle, E. S.; Gomperts, R.; Martin, R. L.; Fox, D. J.; Binkley, J. S.; Defrees, D. J.; Baker, J.; Stewart, J. P.; Head-Gordon, M.; Gonzalez, C.; Pople, J. A. *Gaussian 94*, revision D.4; Gaussian, Inc.: Pittsburgh, PA, 1995.
(27) The $[VO(bpb)]_x$ was formed from the unavoidable contamination of the reaction mixture with atmospheric oxygen during the long reflux time required for the completion of the reaction, and it is insoluble in most common organic solvents.

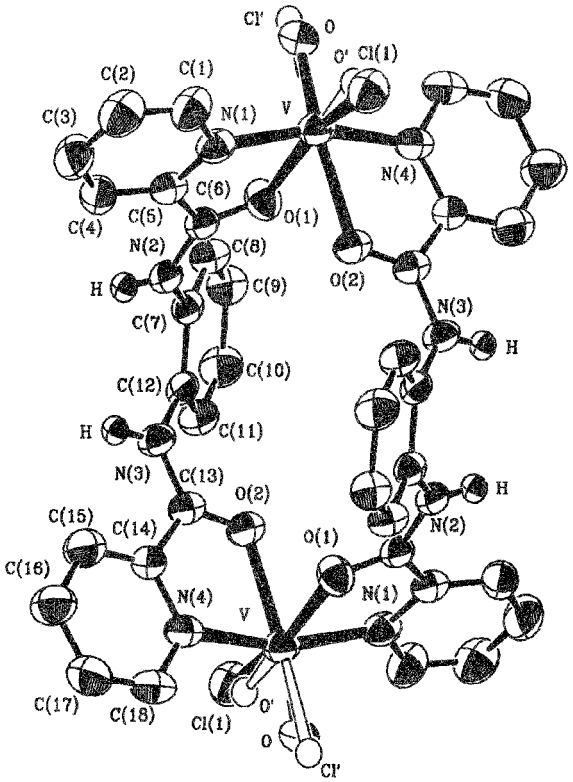

Figure 1. ORTEP diagram of **4**·1.04CH_3OH·1.23thf·0.74H_2O with 50% thermal probability ellipsoids showing atomic numbering scheme.

synthesis to **2**·2$CHCl_3$ has yet to be determined, and further characterization was not pursued.

When **1** is dissolved in nitromethane and exposed to air, it gives the dimeric species **3**·2CH_3NO_2,

$$2NHEt_3[VCl_2(bpb)] + H_2O + \frac{1}{2}O_2 \rightarrow [VOCl(Hbpb)]_2 + 2NHEt_3Cl \quad (1)$$

which is evidently the result of hydrolysis−oxidation of **1**. Reflux of a methyl alcohol solution containing an equivalent of [$VOCl_2$(thf)$_2$], an equivalent of H_2bpb, and 10 equiv of Et_3N gives **5**·CH_3OH, and reflux of a methyl alcohol solution containing a suspension of an equivalent of [$VO(CH_3COO)_2]_x$ and an equivalent of H_2bpb in dimethylformamide gives **5**. The preparation of compound **5** in ca. 40% yield has previously been reported by Cornman and co-workers[12b] by a different method. The synthesis of **5** reported herein gives higher yields (∼80%). When **5**·CH_3OH is dissolved in dimethyl sulfoxide and exposed to air, green crystals of **6**·0.5dmso·0.36CH_3OH·0.13H_2O are formed after about a month. With the formation of the green crystals, white crystals of H_2bpb are formed as well presumably because of hydrolysis of $[VO(bpb)]_x$.

Description of the Structures. The structure of **4** was reported separately[14a] during the course of our studies; therefore, we will give an abbreviated description herein. Compound **4**·1.04CH_3OH·1.23thf·0.74H_2O consists of cationic dimers, [VOCl-(μ_2-η^4-H_2bpb)]$_2^{2+}$, which are neutralized by two chlorine ions. An ORTEP diagram of the cation of **4**·1.04CH_3OH·1.23thf·0.74H_2O is given in Figure 1, while selected bond distances and angles are listed in Table 2. The two vanadium(IV) atoms are centrosymmetrically related and bridged by two neutral H_2bpb ligands. Each vanadium(IV) atom has a distorted octahedral coordination environment consisting of two trans pyridine nitrogens and two cis amide oxygen atoms of two bisbidentate bridging H_2bpb ligands, a chlorine atom, and an oxo group. The six aromatic rings of the two H_2bpb ligands point alternately in opposite directions and define a cylindrical cavity. The axis of the cavity is the *a* axis of the unit cell and thus by translation along the *a* axis "nanotubes" are generated (Figure 2). The disordered methyl alcohol solvents are enclosed in the "nanotubes", while the disordered thf and water solvates fill the space between the tubes. The chlorine counterions are

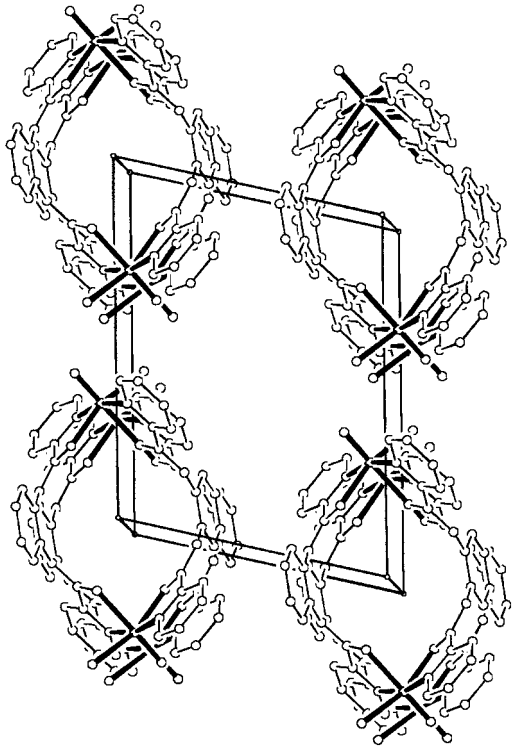

Figure 2. Packing diagram of **4**·1.04CH_3OH·1.23thf·0.74H_2O showing the "nanotubes" formed by the stacking of the cylindrical cavities along the *a* axis of the unit cell.

Table 2. Selected Bond Distances (Å) and Angles (deg) for Compounds **4**·1.04CH_3OH·1.23thf·0.74H_2O and **6**·0.5dmso·0.36CH_3OH·0.13H_2O

Compound **4**·1.04CH_3OH·1.23thf·0.74H_2O			
V−O	1.593(6)	V−N(4)	2.109(5)
V−O(2)	2.169(4)	V−N(1)	2.116(5)
V−O(1)	2.078(4)	V−Cl	2.298(2)
O−V−O(1)	99.0(2)	O−V−N(4)	93.4(3)
O(1)−V−N(4)	92.1(2)	O−V−Cl	100.8(2)
O−V−N−(1)	98.0(3)	O(1)−V−Cl	158.7(1)
O(1)−V−N(1)	76.4(2)	N(4)−V−Cl	94.6(1)
N(4)−V−N(1)	164.9(2)	N(1)−V−Cl	93.0(1)
O−V−O(2)	167.4(3)	O(2)−V−Cl	84.0(1)
O(1)−V−O(2)	78.3(2)	N(4)−V−O(2)	74.5(2)
N(1)−V−O(2)	93.3(2)		
Compound **6**·0.5dmso·0.36CH_3OH·0.13H_2O			
V−O	1.607(2)	V−Ow	2.241(2)
V−N(1)	2.151(2)	V−N(3)	2.014(2)
V−N(2)	2.015(2)	V−N(4)	2.148(2)
O−V−N(3)	105.1(1)	N(2)−V−N(1)	78.1(1)
O−V−N(2)	105.3(1)	N(4)−V−N(1)	119.2(1)
N(3)−V−N(2)	79.5(1)	O−V−Ow	163.2(1)
O−V−N(4)	93.9(1)	N(3)−V−Ow	87.8(1)
N(3)−V−N(4)	78.4(1)	N(2)−V−Ow	87.3(1)
N(2)−V−N(4)	153.8(1)	N(4)−V−Ow	78.1(1)
O−V−N(1)	93.1(1)	N(1)−V−Ow	78.5(1)
N(3)−V−N(1)	154.2(1)		

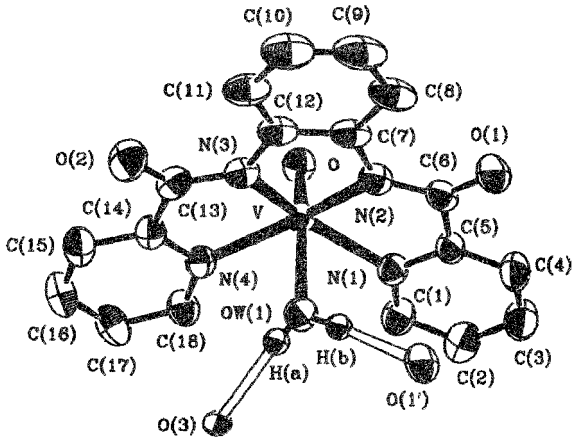

Figure 3. ORTEP diagram of **6**·0.5dmso·0.36CH_3OH·0.13H_2O with 50% thermal probability ellipsoids showing atomic numbering scheme.

strongly H-bonded to the amide hydrogen atoms HN(2) and HN(3) [HN(2)···Cl(2) = 2.284 Å, N(2)···Cl(2) = 3.138 Å, N(2)−HN(2)···Cl(2) = 156.8° and HN(3)···Cl(2′) = 2.343 Å, N(3)···Cl(2′) = 3.140 Å, N(3)−HN(3)···Cl(2′) = 154.9°; Cl(2′) is derived by the $-x$, $2 - y$, $-z$ symmetry operation], while a number of interatomic interactions between the disordered solvent molecules as well as the counterions indicate the presence of an H-bonded network.

The molecular structure of **6**·0.50dmso·0.36CH_3OH·0.13H_2O is shown in Figure 3, while selected bond distances and angles are listed in Table 2. The coordination geometry around vanadium is distorted octahedral. The equatorial positions are occupied by two deprotonated amide nitrogens and two pyridine nitrogen atoms, while the axial positions are occupied by the oxo group and a water molecule. The vanadium atom sits above the best mean plane of the four nitrogen atoms of the planar bpb^{2-} ligand, 0.30 Å toward the oxo group. The ranges of cis and trans angles at the metal center are 78.1(1)°−119.2(1)° and 153.8(1)°−163.2(1)°, respectively.

Of the four V−N bonds, the bonds to N(2) [2.015(2) Å] and N(3) [2.014(2) Å], the amide nitrogens, are in the usual range for $V^{IV}O^{2+}$−diamidate compounds [mean $d(V-N_{am}) = 2.014$ Å][11a,12a,b] while the bond lengths to N(1) [2.151(2) Å] and N(4) [2.148(2) Å], the pyridine nitrogens, are ca. 0.04 Å longer than in similar oxovanadium(IV) compounds containing $V-N_{py}$ bond(s) [average $d[V-N_{py}) = 2.1$ Å].[11a] This difference arises from the increased strain by the bpb^{2-} ligand, as is evident from the $N_{py}-V-N_{py}$ angle, which deviates from 90° (perfect octahedron) to 119.2(1)°. The V═O [1.607(2) Å] and $V-OH_2$ [2.241(2) Å] distances are normal, since in mononuclear octahedral $V^{IV}O^{2+}$ species containing the unit *trans*-V^{IV}(═O)-(OH_2)[28] these distances range from ∼1.58 to 1.59 Å and from ∼2.18 to 2.33 Å with mean distances of ∼1.59 and 2.24 Å, respectively. The strong trans influence of O^{2-} results in the elongation of the $V-OH_2$ bond by ca. 0.2 Å relative to the oxovanadium(IV) species containing the unit *cis*-V^{IV}(═O)-(OH_2)[12e,29] with an average length of 1.60 and 2.03 Å for d(V═O) and $d(V-OH_2)$, respectively. At this point, it is worth noting that the $OV^{IV}-OH_2$ distances are comparable with the $OV^{IV}-O_{amide}$ distances; thus, for the units *trans*-V(═O)(O_{amide}) and *cis*-V(═O)(O_{amide}) the mean $V^{IV}-O_{am}$ values are ∼2.20 and ∼2.00, respectively.[11d,12e,f,30]

The coordinated water molecule is strongly hydrogen-bonded to a carbonyl oxygen O(1′) of a neighboring chelate molecule [OW(1)−H = 0.923 Å, H···O(1′) = 1.794 Å, OW(1)···O(1′) = 2.174 Å, OW(1)−H···O(1′) = 174.1°]. This hydrogen bond results in the formation of a 1-D polymeric structure. Two more contacts between the ligated water molecule and the lattice-disordered dmso and H_2O molecules are observed, and they can be considered as hydrogen bonds despite the disorder of the lattice dmso and H_2O molecules [OW(1)−H = 0.662 Å, H···O_{dmso} = 2.002 Å, OW(1)···O_{dmso} = 2.656 Å, OW(1)−H···O_{dmso} = 169.7°].

Infrared Spectroscopy. Assignments of some characteristic bands are given in Table 3. Compound **6**·0.5dmso·0.36CH_3-OH·0.13H_2O exhibits a medium-intesity band at 3246 cm^{-1}, which is assigned to υ(OH) of coordinated water molecule.[31] The broadness and low frequency of this band are both indicative of hydrogen bonding. Compounds **5**·CH_3OH and **6**·0.5dmso·0.36CH_3OH·0.13H_2O exhibit broad stretching bands of weak intensity at 3475 and 3456 cm^{-1}, respectively, due to υ(O−H) of solvate methyl alcohol.

Differences between the spectra of H_2bpb and its vanadium compounds are readily noticeable in the regions of the υ(NH), amide I, II, III, and δ(py) vibrations. The $\upsilon(NH)_{amide}$ band is absent in the spectra of **1**, **5**·CH_3OH, and **6**·0.5dmso·0.36CH_3-OH·0.13H_2O, as expected from the stoichiometry. In **4**·2thf, the amide I peaks shift to a lower frequency while the amide II and III bands shift to higher frequencies compared to those of free ligand (Table 3). These shifts are consistent with the secondary O_{amide} mode of coordination,[32] established by X-ray crystallography (Figure 1). In the spectra of the fully amide-deprotonated compounds **1**, **5**·CH_3OH, and **6**·0.5dmso·0.36CH_3-OH·0.13H_2O the amide II and III peaks are replaced by a medium to strong band at 1342−1360 cm^{-1}. This replacement is to be expected because the removal of the amide protons produces a pure C−N stretch. The more complicated IR spectra of **3**·2CH_3NO_2 clearly indicate the simultaneous presence of both neutral and deprotonated amide groups, in accord with the single-crystal X-ray structure of it (Figure 4C). The amide I, II, and III bands at 1652, 1528, and 1296 cm^{-1}, respectively, follow the shift pattern observed for **4**·2thf, while the υ(C═O) and υ(C−N) modes of the deprotonated amide group at 1622 and 1384 cm^{-1}, respectively, follow the shift pattern observed for **1**.

The band at 620 cm^{-1} in the free ligand, attributable to the in-plane deformation of the pyridine ring, shifts to higher frequency in its vanadium compounds, thus indicating ligation of the pyridine nitrogen atoms[33] of H_2bpb to vanadium.

(28) (a) Mohan, M.; Bond, M. R.; Otieno, T.; Carrano, C. J. *Inorg. Chem.* **1995**, *34*, 1233. Letho, J. Z.; Samuel, E.; Dromzee, Y.; Jeannin, Y. *Inorg. Chim. Acta* **1987**, *126*, 35. (b) Zah-Letho, J.; Samuel, E.; Dromzee, Y.; Jeannin, Y. *Inorg. Chim. Acta* **1987**, *126*, 35. (c) Priebsch, W.; Rehder, D. *Inorg. Chem.* **1990**, *29*, 3013. (d) Cavaco, I.; Pessoa, J. C.; Duarte, M. T.; Gillard, R. D.; Matias, P. *Chem. Commun.* **1996**, 1365.

(29) (a) Uoi, S.; Nishizawa, M.; Matsumoto, K.; Kuroya, H.; Saito, K. *Bull. Chem. Soc. Jpn.* **1979**, *52*, 452. (b) Demsar, A.; Sukovec, P. *J. Fluorine Chem.* **1984**, *24*, 369. (c) Sundheim, A.; Mattes, R. *Z. Naturforsch.* **1993**, *48b*, 125. Hazell, A.; McKenzie, C. J.; Moubaraki, B.; Murray, K. S. *Acta Chem. Scand.* **1997**, *51*, 470. Kanamori, K.; Ino, K.; Okamoto, K. *Acta Crystallogr.* **1997**, *C53*, 672. (d) De Munno, G.; Bazzicalupi, C.; Focus, J.; Loret, F.; Julve, M. *J. Chem. Soc., Dalton Trans.* **1994**, 1879. (e) Mahroof-Tahir, M.; Keramidas, A. D.; Goldfarb, R. B.; Anderson, O. P.; Miller, M. M.; Crans, D. C. *Inorg. Chem.* **1997**, *36*, 1657. (f) Boasck, U.; Knopp, P.; Habenicht, C.; Wieghardt, K.; Bernhard, N.; Weiss. J. *J. Chem. Soc., Dalton Trans.* **1991**, 3165.

(30) Kabanos, T. A.; Keramidas, A. D.; Papaioannou, A. B.; Terzis, A. *Inorg. Chem.* **1994**, *33*, 845.

(31) Nakamoto, K. *Infrared and Raman Spectra of Inorganic and Coordination Compounds*, 4th ed.; Wiley: New York, 1986.

(32) Barnes, D. J.; Chapman, R. L.; Stephens, F. S.; Vagg, R. S. *Inorg. Chim. Acta* **1981**, *51*, 155.

(33) Clark, R. J. H.; Williams, C. S. *Inorg. Chem.* **1965**, *4*, 350.

Table 3. Characteristic Infrared Bands (cm^{-1}) of H_2bpb and Its Vanadium Compounds

compound	infrared bands							
	ν(NH)	amide I[a]	amide II[b]		amide III[b]	ν(V=O)	ν(V−Cl)	δ(py)[c]
H_2bpb	3316s, 3260sh	1676vs	1516vs		1278w			620m
1		1618s		1342s[d]			330m	652w
3·2CH_3NO_2	3078mb	1652vs	1528s		1296m	978vs	370s	656m
		1622m		1384s[d]				
4·2thf	3200m	1644vs, 1626s	1558s		1286w	982s	370m,355m	654m
5·CH_3OH		1630s		1360s[d]		846vs		654w
6·0.5dmso·0.36CH_3OH·0.13H_2O		1624m		1360s[d]		956s		652w

[a] ν(V=O). [b] In secondary amides these bands arise from coupled ν(CN) and δ(NH) modes. [c] In-plane pyridine ring deformation. [d] This is a pure $\nu(C-N)_{amide}$ mode (see text).

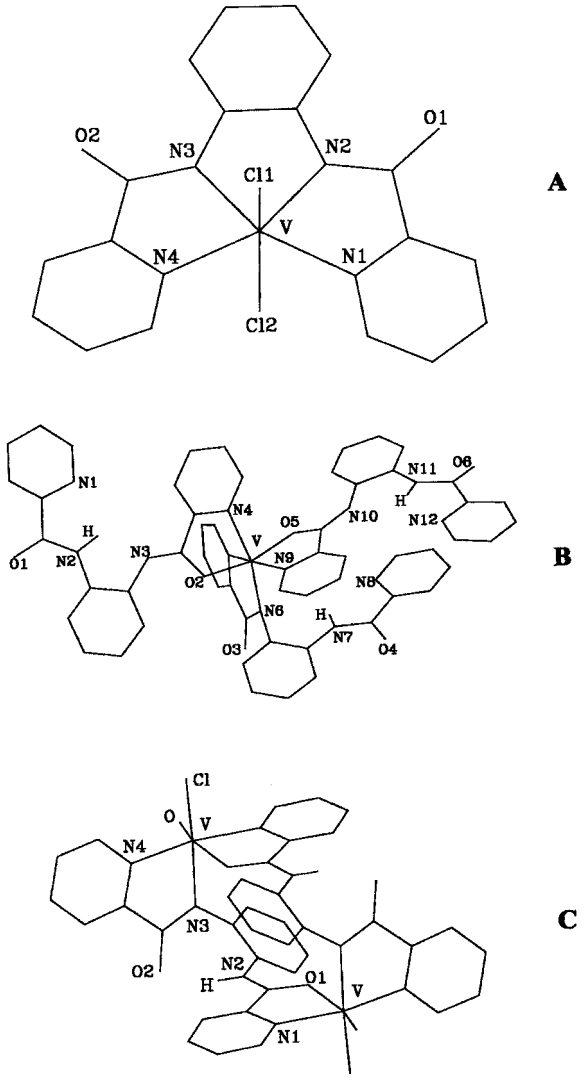

Figure 4. Schematic drawings of **1** (A), **2**·2$CHCl_3$ (B), and **3**·2CH_3NO_2 (C).

The V=O stretching frequency in **3**·2CH_3NO_2, **4**·2thf, and **6**·0.5dmso·0.36H_2O·0.13H_2O ranges from 982 to 956 cm^{-1} (Table 3). The very strong band at 842 cm^{-1} in **5**·CH_3OH arises from the bridging ···V=O···V=O··· stretching vibration,[34] indicating an O-bridged polymeric structure.

Conductivity. A solution of **1** in dichloromethane (1×10^{-3} M) registered a molar conductivity of 1.5 compared to 31 Ω^{-1} cm^2 mol^{-1} for [(*n*-Bu)$_4$N]PF_6 at the same concentration at 25 °C. **1** is a nonelectrolyte in dichloromethane because of strong hydrogen bonding between the counterion ($NHEt_3^+$) and the carbonyl oxygen atom, O(1) (Figure 4A). The molar conductance of **1** in acetonitrile at 25 °C and 1×10^{-3} M concentration is 100 compared to 160 Ω^{-1} cm^2 mol^{-1} for [(*n*-Bu)$_4$N]PF_6 at the same concentration at 25 °C, and this indicates a substantial degree of dissociation of the $NHEt_3^+$ counterion. Note that dichloromethane as a solvent would favor association of $[V^{III}Cl_2(bpb)]^-$ with $[NHEt_3^+]$ much more strongly than would acetonitrile because of both the difference in dielectric constants and the difference in their nucleophilicities. Compound **5**·CH_3OH is a nonelectrolyte in dmso.

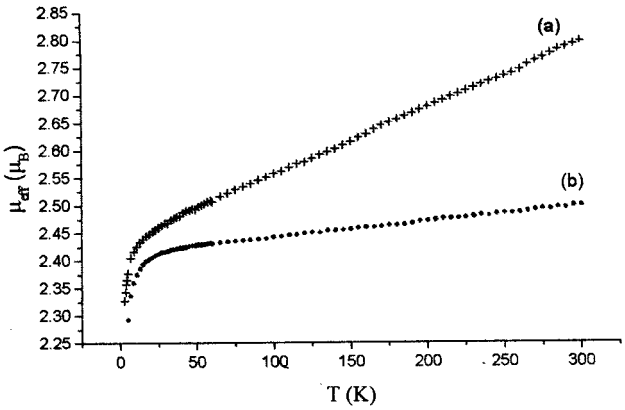

Figure 5. Plot of μ_{eff} vs T for complexes **3**·2CH_3NO_2 (a) and **4**·2thf (b). The solid line is a fit of the data to the appropriate equation; see the text for fitting parameters.

Magnetic Susceptibility and EPR Studies. Variable-temperature solid-state magnetic susceptibility data were collected on powdered samples of complexes **3**·2CH_3NO_2 and **4**·2thf in a 6.0 kG applied magnetic field and in the temperature ranges 3.0−300 K and 5.0−300 K, respectively.

Both complexes behave similarly; there is a steady decrease of μ_{eff} with decreasing temperature, from 2.79 μ_B at 300 K to 2.33 μ_B at 3 K for **3**·2CH_3NO_2 and 2.50 μ_B at 300 K to 2.30 μ_B at 5 K for **4**·2thf. The decrease becomes sharper at ∼17 K for **3**·2CH_3NO_2 and at ∼25 K for **4**·2thf. The μ_{eff} vs T data are shown in Figure 5 for both **3**·2CH_3NO_2 and **4**·2thf.

The data were fit to the Bleany−Bowers[35] equation based on the zero-field spin Hamiltonian $\hat{H} = -2J\hat{S}_1\hat{S}_2$ and corrected for the presence of temperature-independent paramagnetism (TIP) and mononuclear impurities:

$$X_M = \frac{2Ng^2\mu_B^2}{kT}\left[\frac{1}{3+\exp(2x)}\right](1-\rho) + \frac{\rho Ng^2\mu_B^2}{4kT} + \text{TIP} \quad (2)$$

where $x = -J/(kT)$, N is Avogadro's number, ρ is the mole

(34) (a) Mathew, M.; Carty, A.; Palenik, G. J. *J. Am. Chem. soc.* **1970**, *92*, 3197. (b) Kasahara, R.; Tsuchimoto, M.; Ohba, S.; Nakajima, K.; Ishida, H.; Kojima, M. *Inorg. Chem.* **1996**, *35*, 7661.

(35) Bleany, B.; Bowers, K. D. *Proc. R. Soc. London, Ser. A* **1952**, *214*, 451.

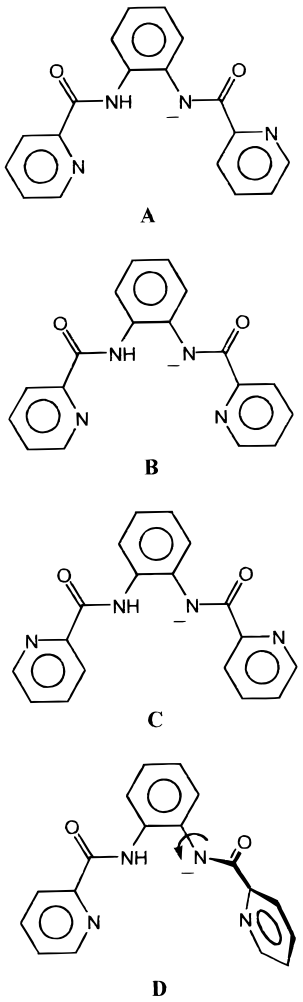

Figure 6. Optimized conformers of Hbpb$^-$ ligand (**A**, **B**, **C**) and its nonplanar structure **D** at the HF level.

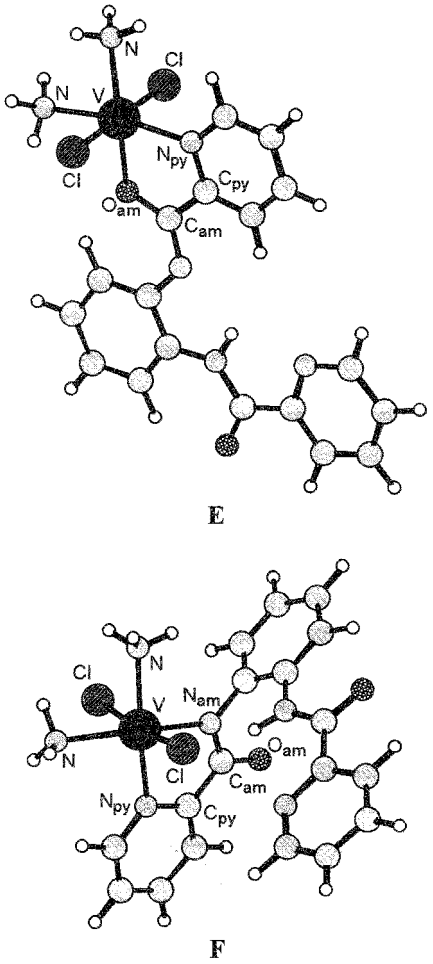

Figure 7. Ab initio optimized geometries of model complexes {VCl_2-$(NH_3)_2$[η^2-(N_{py},O_{am})−Hbpb]} (**E**) and {$VCl_2(NH_3)_2$[η^2-(N_{py},N_{am})−Hbpb]} (**F**) at the HF level.

fraction of mononuclear impurity, and the other symbols have their usual meaning.

Data were satisfactorily fit into eq 2 with $J = -0.36$ cm^{-1}, $g = 1.99$, $\rho = 0.0061$, TIP $= 774 \times 10^{-6}$ emu mol^{-1}, $R = 5.4 \times 10^{-6}$ for **3**·2CH_3NO_2 and $J = -0.67$ cm^{-1}, $g = 1.98$, $\rho = 0.0064$, TIP $= 145 \times 10^{-6}$ emu mol^{-1}, $R = 3.0 \times 10^{-6}$ for **4**·2thf, where R is the quality of the fit defined by

$$R = \frac{\sum[(\chi T)_{exp} - (\chi T)_{calc})]^2}{\sum(\chi T)_{exp}{}^2}$$

The high-temperature spin-only value of μ_{eff} for a d^1-d^1 system with isotropic $g = 2.0$ is expected to be 2.45 μ_B. The low-temperature behavior of μ_{eff} for both complexes is as expected for a d^1-d^1 system; at higher temperatures the μ_{eff} vs T behavior of both complexes is modified by the presence of TIP. The value of TIP for **3**·2CH_3NO_2 is exceptionally high, though similar values have been reported.[36]

The solid-state powder EPR spectra at liquid helium temperature of both complexes exhibit an isotropic signal centered at $g \approx 2.0$. The temperature dependence of the line intensity in the temperature range 4.0−40 K indicates small antiferromagnetic interactions, as shown clearly by susceptibility studies. EPR studies were attempted in frozen solutions of **3**·2CH_3NO_2 in CH_3OH and **4**·2thf in CH_3OH, but for both cases the line shape was not preserved. The EPR spectra taken were typical of mononuclear oxovanadium(IV) molecules.

Ab Initio Calculations. The ab initio study started from the optimization of a series of low-energy conformers of the free ligand Hbpb$^-$, shown in Figure 6, at the HF level. The conformer with the lowest energy, **A**, is very similar to the structure of the η^2-(N_{py},O_{am})−Hbpb$^-$ ligand found in the complex **2**·2$CHCl_3$ (Figure 4B). The remaining two planar conformers, **B** and **C**, are located at 2.4 and 3.9 kcal/mol above **A**. A structure analogous to the η^2-(N_{py},N_{am}) mode of coordination of the Hbpb$^-$ ligand in the actual complex, **D**, has been found to be 23.7 kcal/mol higher than **A**. It is distorted from planarity, as shown in the structure of the complex (Figure 4B), with the deprotonated pyridinecarboxamide group forming an angle of 70° with the rest of the molecule. It is not a minimum on the potential energy surface, and an optimization started from this structure gave the conformer **A**. This shows that the ligation of the ligand in a η^2-(N_{py},N_{am}) mode involves a significant deformation energy.

Because of the large size of the complex, the study of the two different modes of coordination of the ligand Hbpb$^-$ was done by means of ab initio calculations on the two model complexes, namely, {$VCl_2(NH_3)_2$[η^2-(N_{py},O_{am})−Hbpb]} and {$VCl_2(NH_3)_2$[η^2-(N_{py},N_{am})−Hbpb]} where there is only one Hbpb$^-$ in either its η^2-(N_{py},O_{am}) or its η^2-(N_{py},N_{am}) coordination mode, and the octahedral coordination sphere was completed

(36) Rambo, J. R.; Castro, S. L.; Folting, K.; Bartely, S. L.; Heintz, R. A.; Christrou, G. *Inorg. Chem.* **1996**, *35*, 6844.

Table 4. Selected ab Initio Optimized Geometrical Parameters (Distances and Angles) for the Chelate Rings[a] of $\{VCl_2(NH_3)_2[\eta^2\text{-}(N_{Py},O_{Am})-Hbpb]\}$ and $\{VCl_2(NH_3)[\eta^2\text{-}(N_{Py},N_{Am})-Hbpb]\}$ Model Complexes Compared to the Experimental Parameters of $\eta^2\text{-}N_{Py},O_{Am}$ and $\eta^2\text{-}N_{Py},N_{Am}$ Modes of Coordination, Respectively[b]

	calcd		exptl	
	model $\eta^2\text{-}N_{py},O_{am}$	model $\eta^2\text{-}N_{py},N_{am}$	ligands $\eta^2\text{-}N_{py},O_{am}$	ligand $\eta^2\text{-}N_{py},N_{am}$
$V-O_{am}$	2.090		1.955[c]	
$V-N_{py}$	2.196	2.149	2.149	2.119
$V-N_{am}$		1.977		2.011
$N_{py}-V-O_{am}$	77.02		77.54	
$N_{py}-V-N_{am}$		82.81		79.35
$V-N_{py}-C_{py}$	113.26	108.49	113.44	112.63
$N_{py}-C_{py}-C_{am}$	144.58	116.45	113.31	116.28
$C_{py}-C_{am}-O_{am}$	116.98		114.43	
$C_{py}-C_{am}\text{-}-_{am}$		116.65		112.88
$C_{am}-O_{am}-V$	118.16		120.72	
$C_{am}-N_{am}-V$		118.89		118.15

[a] Atom labels are given in **E** and **F** (Figure 7). [b] Bond distances are given in Å, and angles in deg. [c] Mean values of the two ligands with the $\eta^2\text{-}N_{py},O_{am}$ mode of ligation.

by two chlorine atoms and two molecules of NH_3. The geometry of the two model complexes has been fully optimized under no symmetry constraints (point group C_1) at the HF level. The optimized geometries **E** and **F** are shown in Figure 7, whereas the optimized geometrical parameters (distances and angles) concerning the two chelate rings shown in Figure 7 are given in Table 4.

There is an apparent overall agreement between the calculated geometries with those found experimentaly for both types of coordination. In the $\{VCl_2(NH_3)_2[\eta^2\text{-}(N_{py},O_{am})-Hbpb]\}$ model, **E**, the ligand is almost planar, whereas in $\{VCl_2(NH_3)_2[\eta^2\text{-}(N_{py},N_{am})-Hbpb]\}$, **F**, the ligand is distorted from planarity, with the deprotonated pyridinecarboxamide group forming an angle of 75° with the rest of the ligand, that is, very close to the experimental angle of 70°. The energy difference of the two model complexes is very little, with **E** lying only 3.3 kcal/mol above **F**. Thus, it seems that the $\eta^2\text{-}(N_{py},N_{am})$ mode of coordination of the ligand is energetically favored. This is also reflected in the fact that the binding energy of the ligation of $[\eta^2\text{-}(N_{py},N_{am})-Hbpb]^-$ and $[VCl_2(NH_3)_2]^+$ fragments is calculated to be 12.4 kcal/mol higher than those of the $[\eta^2\text{-}(N_{py},O_{am})-Hbpb]^-$ and $[VCl_2(NH_3)_2]^+$ fragments. Furthermore, single-point calculations at the HF level of the ligand structures found in the models showed that the $[\eta^2\text{-}(N_{py},O_{am})-Hbpb]^-$ ligand in **E** is 7.6 kcal/mol more stable than the $[\eta^2\text{-}(N_{py},N_{am})-Hbpb]^-$ ligand in **F**, and this is mainly due to the distortion from planarity. Therefore, the small energy difference of the two model complexes can be easily understood if we take into account that the coordination of $Hbpb^-$ in an $\eta^2\text{-}(N_{py},N_{am})$ mode of ligation has an energy cost of 7.6 kcal/mol relative to the $\eta^2\text{-}(N_{py},O_{am})$ mode of ligation. This deformation energy is counterbalanced by a stronger interaction of the ligand with the $\eta^2\text{-}(N_{py},N_{am})$ coordination, giving an energy for **F** that is slightly lower that that of **E**. The question that arises now is why only one of the three $Hbpb^-$ ligands in the actual complex $\{V[\eta^2\text{-}(N_{py},O_{am})-Hbpb]_2[\eta^2\text{-}(N_{py},N_{am})-Hbpb]\}\cdot 2CHCl_3$ (Figure 4B) adopts the energetically preferred $\eta^2\text{-}(N_{py},N_{am})$ coordination mode and the other two the $\eta^2\text{-}(N_{py},O_{am})$ one. An examination of the model complexes $\{V[\eta^2\text{-}(N_{py},O_{am})-Hbpb][\eta^2\text{-}(N_{py},N_{am})-Hbpb]_2\}$ and $\{V[\eta^2\text{-}(N_{py},N_{am})-Hbpb]_3\}$ showed that the coordination of a second or third ligand in the stronger $\eta^2\text{-}(N_{py},N_{am})$ mode is not possible because of large steric hindrance. In conclusion, the structure adopted experimentally is a result of a fine balance of the ligand deformation energy, the relative strength of each coordination mode, and steric hindrance.

Conclusions

In conclusion, novel vanadium(III) and oxovanadium(IV) compounds with the diamidate ligand H_2bpb were synthesized and structurally and physicochemically characterized. H_2bpb is a structurally very versatile ligand, capable of supporting a wide variety of complex stoichiometries and geometries. The doubly deprotonated ligand, bpb^{2-}, acts as a planar tetradentate bis[*N*-amidate-*N*-pyridine] equatorial ligand. The singly deprotonated ligand $Hbpb^-$ behaves as μ_2-bridging-η^4-$(N_{py},O_{am}-N_{py},N_{am})$ and as (N_{py},O_{am}) or (N_{py},N_{am}) chelator, while the neutral ligand H_2bpb behaves as μ_2-bridging-η^4-bis(N_{py},O_{am}) chelator.

Compound **2**·$2CHCl_3$ represents a rare example,[14b,37] the first known for vanadium, of a deprotonated amide coordinated via oxygen and not nitrogen. Ab initio calculations have shown that the structure adopted by **2**·$2CHCl_3$ is a result of a fine balance of the ligand deformation energy, the relative strength of each coordination mode, and steric hindrance. This X-ray structure provides the first solid-state evidence that the $V-O_{amide}$ binding of the $-CON^-$ functionality is a possible mode of ligation in vanadoproteins and in metal−proteins in general, where steric hindrance is a quite common effect.

Acknowledgment. We gratefully acknowledge the support of this research by the Greek General Secretariat of Research and Technology (Grant No. 1807/95), Agricultural Bank of Greece (A.T.E.), Mr. John Boutaris for financial support to A.T., and Mrs. F. Masala for typing this manuscript.

Supporting Information Available: Tables listing atomic positional ($\times 10^4$) parameters of non-H atoms, positional and isotropic thermal parameters of the hydrogen atoms, anisotropic thermal parameters of the non-H atoms, bond lengths, and bond angles associated with compounds **4**·$1.04CH_3OH$·$1.23thf$·$0.74H_2O$ and **6**·$0.5dmso$·$0.36CH_3OH$·$0.13H_2O$. This material is available free of charge via the Internet at http://pubs.acs.org.

IC990837Z

(37) Scheller-Krattiger, V.; Scheller, K. H.; Sinn, E.; Martin, R. B. *Inorg. Chim. Acta* **1982**, *60*, 45.